A Proposed FM Phototube for Demodulating Microwave-Frequency-Modulated Light Signals*

S. E. HARRIS† AND A. E. SIEGMAN†, MEMBER, IRE

Summary—A microwave phototube for demodulating frequency-modulated light signals is proposed. The demodulation is based upon the conversion of the frequency-modulated light into space-modulated light via an optical dispersing element. This space-modulated light is then incident on a photocathode where it is the source of transverse electron beam waves. A complete spectral analysis of the demodulation process is presented. It is shown that a quasi-steady-state viewpoint, *i. e.*, that of an optical signal with slowly varying frequency is permissible only if the optical resolution is sufficiently low. Design parameters for a phototube based on the use of a Michelson echelon are presented. A related scheme employing a Fabry-Perot etalon is also discussed.

Introduction

EXTREMELY BROADBAND optical communications channels may become possible, using the light outputs from coherent optical maser oscillators, if techniques can be developed for modulating and demodulating light signals at high modulation frequencies. For the present, "high modulation frequencies" can be taken to mean microwave frequencies. As contribution towards solving the demodulation problem, we propose in this paper two related and novel schemes for detecting and demodulating optical signals which are frequency modulated (or phase modulated) at a microwave modulating frequency.

The basic method proposed involves converting the optical frequency modulation into space modulation via an optical dispersing element, and then converting the space modulation into transverse electron beam-wave excitation via a photocathode. A schematic of the demodulating scheme is shown in Fig. 1. If the nominally monochromatic light beam incident upon the prism from the upper right in Fig. 1 is frequency modulated, then the ray angle of the light emerging from the prism and the position of the light spot on the photocathode will be correspondingly modulated. The motion of the light spot on the photocathode will produce an initial transverse position modulation of the electron beam, *i.e.*, it will excite transverse waves on the beam at the modulation frequency. In microwave-tube terminology, the so-called synchronous cyclotron waves are excited. This transverse wave excitation can then be amplified and detected in the FM phototube by a wide variety of means which are well known in the microwave electron tube field. The eventual result will be a microwave output from the FM phototube which duplicates the frequency modulation on the incident light signal.

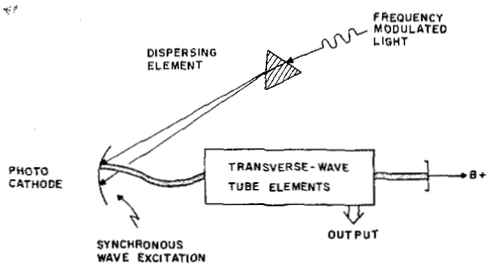

Fig. 1—Schematic of discriminator phototube.

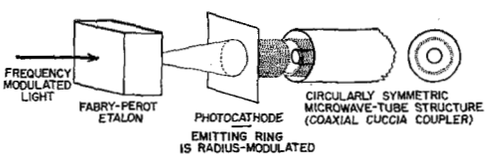

Fig. 2—Fabry-Perot FM phototube.

The preceding description is, in reality, a simplified and not entirely correct description of how the demodulation process operates. We give a more rigorous mathematical description below. Two types of dispersing elements commonly used in interferometry which are suited for the demodulation process are the Michelson echelon, and the Fabry-Perot etalon. The Michelson echelon will produce a line of light on the photocathode and this line will move up and down in a direction transverse to its length at the modulating frequency. Fig. 2 illustrates the related scheme which is a circularly symmetric variant of the first scheme. In this case, the dispersing element is a Fabry-Perot interferometer, which produces a ring pattern on the photocathode. (For simplicity, a semi-transparent transmission type of photocathode is shown in the drawing.) The ring or series of rings on the photocathode produces one or a series of hollow electron beams whose radii are modulated in direct proportion to the frequency modulation of the incident light. The resultant scalloping or radius modulation of the hollow electron beam or beams can be amplified and detected by appropriate circularly symmetric transverse field elements, *e.g.*, coaxial Cuccia couplers helix-on-rod slow-wave circuits, and the like.

This paper first presents a spectral or Fourier analysis of the basic demodulation process, since the "instantane-

* Received March 5, 1962. This work has been supported by the Wright Air Development Division of the U. S. Air Force.
† Electrical Engineering Department, Stanford University, Stanford, Calif.

eous frequency" description just given is not entirely correct. Some practical design formulas for this type of FM phototube are then presented, including design details appropriate to an initial experiment which is now in preparation by the authors. The design calculations indicate that there should not be any great difficulty in experimentally demonstrating this type of FM light demodulation with strong output signals and large signal-to-noise ratio.

It may be noted that the most promising types of microwave-frequency light modulators at the present time use the Kerr or Pockels effects, in which the indices of refraction of liquids or crystals along certain axes are modulated by the application of strong electric fields. Properly oriented linear polarizers are generally used together with such Kerr or Pockels cells in order to obtain amplitude modulation of the light. The Kerr or Pockels cell itself, however, is basically a phase modulator: incident light polarized along certain principal axes will experience pure phase modulation. Thus, pure phase or frequency modulation of an optical signal at a microwave modulation frequency can readily be obtained.

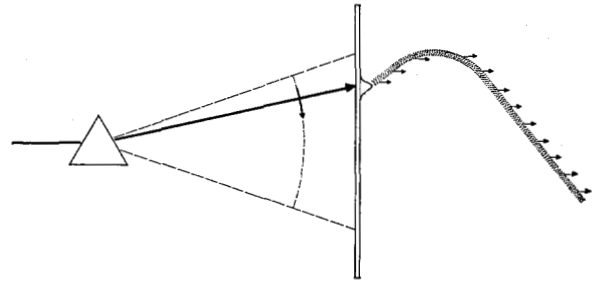

Fig. 3—Variable frequency viewpoint.

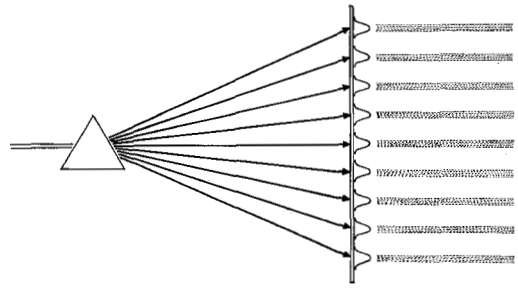

Fig. 4—Spectral viewpoint.

Spectral Analysis

Fig. 3 is another sketch of the essential elements of the demodulation process as seen from the instantaneous frequency point of view. By this, we mean that the instantaneous frequency of the light is taken to be varying at the modulation rate, so that the ray angle of the dispersed light and the position of the beam spot sweep back and forth at the modulation rate. This produces a transversely-modulated electron beam from the semi-transparent photocathode, as illustrated in the figure. This description of the demodulation process must be valid at least in the quasi-steady-state case, where the exact interpretation to be given the term "quasi-steady state" will emerge from the following analysis.

A frequency-modulated signal is more accurately described from a Fourier or spectral viewpoint as consisting of a carrier and a number of sidebands spaced away from the carrier by the modulation frequency. If the demodulation process is approached from this viewpoint, it then appears that Fig. 3 should be replaced by a sketch such as Fig. 4. In Fig. 4, each different sideband or spectral component is dispersed by the prism to a different angle, each producing an individual spot of light on the photocathode, and hence an individual steady beamlet of electrons. Each light ray corresponds to an optical frequency differing by the modulation frequency from the optical frequency of adjacent rays. Moreover, each spectral component, and hence the current in each electron beamlet, should have constant intensity in time, since the cathode does not follow variations at optical frequencies. From this spectral viewpoint, therefore, it may at first appear that the emitted electron beam or beams do not move transversely at all, and the demodulation process will not work.

This apparent paradox is resolved, however, as the following analysis will show in detail, by noting that all of the light rays or light spots will always overlap on the photocathode surface to at least some extent, because of the finite resolving power of the dispersing element. (Fig. 4 has been drawn, however, as if this overlap were very small.) As a result of the inevitable overlap, there will be some photomixing or beating between all the spectral components at all points on the photocathode. As a result of this, the electron emission at each point on the photocathode will contain at least some component at the modulation frequency and also at harmonics of this frequency. The total effect of this, as the following analysis will show, is simply that the *center of gravity* of all the beamlets, *i.e.*, of the total photoemitted current, moves back and forth transversely at the modulation frequency rate. This is all that is required to make the modulation scheme work, since the subsequent transverse-microwave-tube elements respond essentially to the center-of-gravity motion of the total electron stream.

Moreover, the following analysis will show that the transverse deviation of the center of gravity is given in general by the peak deviation which would be predicted by the instantaneous-frequency viewpoint, reduced by a factor of the form sinc $x(\equiv \sin x/x)$ which depends only on the amount of overlap of adjacent spectral components. Therefore, no matter how low the modulation frequency may be, it is still possible (at least in principle) to make the optical resolution so high, *i.e.*, to make the individual light spots so sharp (at fixed dispersion), that the amount

of overlap, the center-of-gravity motion, and hence the demodulation effect, all disappear. To say this in another way, the modulation frequency is "low" enough for the quasi-steady state or instantaneous-frequency viewpoint to be correct only when the individual sidebands are not resolvable by the optical dispersing element employed.

We now present the detailed analysis of this effect, using the spectral viewpoint. Suppose that the amplitude, *e.g.*, the electric field strength, of the modulated light signal incident on the dispersing element is given by

$$e(t) = \exp\left[j(\omega_c t + \delta \sin \omega_m t)\right] = e^{j\omega_c t} \sum_{n=-\infty}^{\infty} J_n(\delta) e^{jn\omega_m t} \tag{1}$$

where ω_c is the optical carrier frequency, ω_m is the modulating frequency, ω_d is the maximum frequency deviation, and $\delta = \omega_d/\omega_m$. Note that since the instantaneous phase of the light is $\phi(t) = \omega_c t + \delta \sin \omega_m t$, an instantaneous frequency can be defined as $\omega(t) = d\phi(t)/dt = \omega_c + \delta\omega_m \cos \omega_m t = \omega_c + \omega_d \cos \omega_m t$. We may also note that $J_n(-\delta) = (-1)^n J_n(\delta)$. We next assume that the amplitude of the light spot on the photocathode surface due to a monochromatic light signal incident upon the dispersing element has the general form or line shape in the x direction

$$U(x) = (N/\pi)^{1/2} \operatorname{sinc} N(x - x_0) \tag{2}$$

where x_0 is the center of the spot. The parameter N is characteristic of the optical dispersing element used. For a grating or similar dispersing element, N is proportional to the number of lines or steps in the grating. This expression for $U(x)$ is actually a large-N approximation to a more exact form, but the approximation is generally valid for most common dispersing elements. The normalization is chosen so that $\int U^2(x)\, dx$ over $-\infty$ to ∞ is unity.

The spot center position x_0 is to a good first approximation linearly related to the optical frequency ω of the incident monochromatic signal. We will choose our coordinate system such that $x_0 = 0$ for the optical-carrier frequency $\omega = \omega_c$, and we will suppose that the optical dispersion of the dispersing element is such that the spot center moves by an amount $\Delta x_0 = a$ for an optical-frequency shift $\Delta\omega = \omega_m$, the modulating frequency. With these assumptions, the total optical amplitude on the photocathode due to the modulated light input of (1) can be written

$$e(x, t) = \sum_{n=-\infty}^{\infty} J_n(\delta) U(x - na) e^{j(\omega_c + n\omega_m)t}. \tag{3}$$

Now, the emitted current density from the photocathode as a function of position and time will be proportional to the square of the above optical amplitude, with the optical-frequency variations removed. Therefore, we can write the current density $j(x, t)$ as

$$j(x, t) = \tfrac{1}{2} e(x, t) e^*(x, t). \tag{4}$$

From the arguments given earlier, we are interested in particular in the motion of the center of gravity of this resulting current density, where this motion is given by

$$\Delta x_{cg}(t) = \frac{\int_{-\infty}^{\infty} x j(x, t)\, dx}{\int_{-\infty}^{\infty} j(x, t)\, dx} = \frac{m(t)}{i(t)} \tag{5}$$

with $m(t)$ being the first moment of the current-density distribution.

The expression $j(x, t) = \frac{1}{2} e(x, t) e^*(x, t)$ contains products of all the optical-frequency terms with each other. This leads to an infinite set of dc terms arising from each optical component beating with itself; an infinite set of modulation frequency or ω_m terms which arise from each optical component beating with its adjacent neighbors; an infinite set of $2\omega_m$ terms which arise from each optical component beating with optical components two away; an infinite set of $3\omega_m$ components; and so on. In these products, two integrals occur repeatedly. These are

$$\int_{-\infty}^{\infty} U(x - a) U(x - b)\, dx = (N/\pi) \cdot \int_{-\infty}^{\infty} \operatorname{sinc} N(x - a) \cdot \operatorname{sinc} N(x - b)\, dx = \operatorname{sinc} N(a - b) \tag{6}$$

$$\int_{-\infty}^{\infty} x U(x - a) U(x - b)\, dx = (N/\pi) \cdot \int_{-\infty}^{\infty} x \operatorname{sinc} N(x - a) \cdot \operatorname{sinc} N(x - b)\, dx = [\operatorname{sinc} N(a - b)](a + b)/2 \tag{7}$$

as may readily be verified by contour integration.

A very useful general result may be obtained from these two integrals: if there is one optical component of amplitude A centered at $x = a$ and another of amplitude B centered at $x = b$, then the complete effect of their product, or of the beating between them, so far as both current and first moment are concerned, is completely accounted for by a delta function or impulse of current density of magnitude 2 *Re* $[AB^*]$ sinc $N(a - b)$ located at $x = (a + b)/2$. Consider, for example, the two overlapping optical components $J_3(\delta)$ sinc $N(x - 3a)$ exp $[j(\omega_c + 3\omega_m)t]$ and $J_4(\delta)$ sinc $N(x - 4a)$ exp $[j(\omega_c + 4\omega_m)t]$. The product of these two components produces a transverse distribution of ac current density at the modulation frequency ω_m, with current amplitude and instantaneous center of gravity given by:

Current contribution

$$= 2J_3(\delta) J_4(\delta) \frac{\sin Na}{Na} \cos \omega_m t. \tag{8}$$

First-moment contribution

$$= 2J_3(\delta)J_4(\delta)\frac{\sin Na\ 7a}{Na\quad 2}\cos\omega_m t. \tag{9}$$

The same current and first-moment contributions would be obtained from a current-density impulse of amplitude $2J_3(\delta)J_4(\delta)$ sinc Na cos $\omega_m t$, located at $x = 7a/2$.

As a result of this, the doubly infinite set of terms implicit in $j(x, t)$ from (3) and (4), and hence also in $i(t)$ and $m(t)$ from (5), can be represented by appropriate sets of impulse functions. The utility of this representation lies in the ease with which various important results can be obtained, as will shortly become apparent. As a first step, from (3), $e(x, t)$ may be represented schematically by a singly infinite set of optical components of magnitude $J_n(\delta)$ and frequency $(\omega_c + n\omega_m)$, located at $x = na$, as shown schematically in Fig. 5(a). The lines run upward or downward in accordance with the positive or negative sign of the corresponding component.

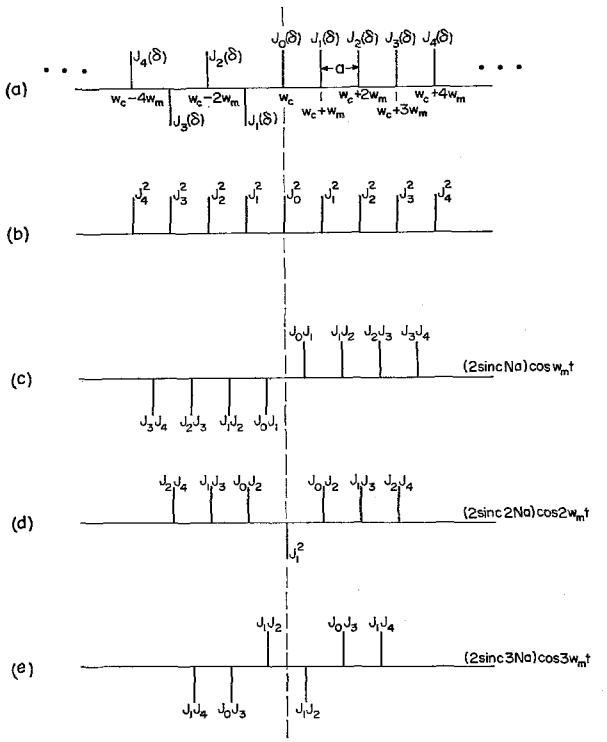

Fig. 5—(a) Optical frequency schematic. (b) Equivalent dc beat picture. (c) Equivalent 1st harmonic beat picture. (d) Equivalent 2nd harmonic beat picture. (e) Equivalent 3rd harmonic beat picture.

We can then obtain first the dc components of $j(x, t)$ by taking all the dc products or beats between the optical components of Fig. 5(a), *i.e.*, the product of each optical component in Fig. 5(a) with itself. According to our rules, this is equivalent to a set of current-density impulses of magnitude $J_n^2(\delta)$, located at $x = na$, as shown in Fig. 5(b).

We can next obtain the fundamental or cos $\omega_m t$ component of $j(x, t)$ by considering the beating between each optical component in Fig. 5(a) and its adjacent neighbors. According to our rules, this yields an infinite set of current-density impulses of value $2J_n(\delta)J_{n+1}(\delta)$ sinc Na, located at $x = (n + 1/2)a$, as shown in Fig. 5(c).

By following the same approach, the $\pm 2\omega_m$, $\pm 3\omega_m$, and all higher harmonic components of $j(x, t)$ can be represented by infinite sets of impulse functions, as illustrated for the $2\omega_m$, and $3\omega_m$ cases in Fig. 5(d) and 5(e). The total current density $j(x, t)$ is then represented by the doubly infinite set of delta functions contained in Fig. 5(b)–(e) and on through all higher harmonics.

The instantaneous current $i(t)$ can be written as a Fourier series, in which only cosine terms occur due to the original choice of the form of the FM signal.

$$i(t) = \sum_{n=-\infty}^{\infty} I_n \cos\omega_m t. \tag{10}$$

It is apparent that each component I_n in the Fourier series is just the summation of all the terms in the corresponding line of Fig. 5. Thus,

$$I_0 = [J_0^2 + 2J_1^2 + 2J_2^2 + \cdots] \tag{11}$$

$$I_1 = I_3 = \text{all odd terms} = 0 \text{ (by symmetry)}$$

$$I_2 = 2 \text{ sinc } N2a[-J_1^2 + 2J_0J_2 + 2J_1J_3 + \cdots]$$

and so on. The summations in this expansion can be compared with the identity

$$\frac{\sin m\pi}{m\pi} = J_m(\delta)J_{-m}(\delta) + 2\sum_{n=1}^{\infty} J_{n+m}(\delta)J_{n-m}(\delta). \tag{12}$$

Inserting integral values of m makes it apparent that all of the ac terms in the current expansion are zero, and the total instantaneous current is given by $i(t) = I_0 = I$. We have thus arrived at the perhaps obvious result that the total current is constant with time; the beating between different components introduces no amplitude modulation of the total current. This checks with our intuition in the quasi-steady state, in which the beam swings back and forth with no variation in amplitude.

We may next express the center-of-gravity motion in a similar Fourier series by writing

$$\Delta x_{cg}(t) = m(t) = \sum_{n=-\infty}^{\infty} M_n \cos\omega_m t \tag{13}$$

and the various frequency components can again be written down very rapidly by inspection of the corresponding line in Fig. (5). Thus, the quantity of major interest, namely, the fundamental frequency component of $\Delta x_{gc}(t)$, is given by the summation of a series of couples of arm length a, 3a, 5a, and so on, from Fig. 5(c). The full expression is

$$M_1 = 2 \text{ sinc } Na[aJ_0(\delta)J_1(\delta) + 3aJ_1(\delta)J_2(\delta) + \cdots]$$

$$= 2a \text{ sinc } Na \sum_{m=0}^{\infty}(2m + 1)J_m(\delta)J_{m+1}(\delta)$$

$$= a\ \delta \text{ sinc } Na \tag{14}$$

where the final step follows from a closed form for the Bessel function series given in the Appendix.

It is apparent from symmetry considerations that all of the even-integer M_n terms are zero. The higher odd-integer M_n terms can be written in general as

$$M_n = 2a \operatorname{sinc} Na \sum_{m=0}^{\infty} (2m+1) J_{m-n}(\delta) J_{m+n+1}(\delta)$$

$$= 0 \qquad n \text{ odd}, \geq 1 \tag{15}$$

where the more general form of the Bessel function sum is proven in the Appendix. We might add that we were first led to these identities from the physical considerations of this problem.

We may note that if an optical-frequency shift $\Delta\omega = \omega_m$ shifts the position of a component by $\Delta x = a$, then an optical-frequency shift of $\Delta\omega = \omega_d$ should shift the spot position by $\Delta x = (\omega_d/\omega_m)a = \delta a$. Therefore, the peak motion of the light spot from the quasi-steady-state instantaneous-frequency viewpoint would be $\Delta x_{qs}^{(i)} = \delta a \cos \omega_m t$. It is apparent from our analysis that the motion of the center of gravity of all the beamlets is given by

$$\Delta x_{cg}(t) = [\delta a \operatorname{sinc} Na] \cos \omega_m t$$

$$= (\operatorname{sinc} Na)\ \Delta x_{qs}(t). \tag{16}$$

In short, as stated earlier, the center-of-gravity motion predicted by the rigorous spectral analysis just equals the motion predicted by the simplified instantaneous-frequency viewpoint, reduced by the factor sinc Na. The reduction factor sinc Na is a measure only of the amount of overlap of adjacent spectral components. The reduction factor approaches unity for large overlap, *i.e.*, low optical resolution and/or low ω_m, but becomes small as soon as the modulating frequency ω_m exceeds the smallest optical-frequency increment resolvable by the dispersing element employed.

It may be instructive to consider in particular the small-δ case, *i.e.*, maximum instantaneous-frequency deviation ω_d small compared to the modulation-frequency ω_m. In this case, only the carrier and the first sideband on each side of it are of sizable amplitude. Then, if the resolution of the optical system is high enough to resolve these components, there will be three distinct light spots on the photocathode. There will be three corresponding distinct electron beamlets, and the demodulation effect will be eliminated or at least greatly reduced. If, however, the optical resolution is not this good, then the three spots will overlap to a substantial degree, and merge into a single total spot. The demodulation effect will then approach its full strength. The center of gravity of the spot, in this case, need move only a small distance compared to the size of the spot to give the full demodulation effect, since $\omega_d \ll \omega_m$.

Discussion

The previous analysis has been in some ways highly simplified, *e.g.*, it assumes completely coherent and parallel plane-wave light incident upon the dispersing element (although this assumption should be quite valid in practical situations making proper use of optical maser sources). Ideal dispersing elements are also assumed. The resolution referred to in the discussion is then the ultimate theoretical resolution of the optical system employed. Of course, in practice, the actual optical resolution in an experiment may be much poorer than the ultimate theoretical resolution, for a variety of practical reasons. In general the resolution is deteriorated because of effects which cause a spread in the values of the center position x_0 of any given monochromatic light component. This effectively broadens the spot size and deteriorates the resolution. We will refer to such spot broadening effects as system broadening, in contrast to the ultimate theoretical broadening due only to diffraction effects.

Now, we argue that so long as any system broadening effects act equally on all spectral components (*e.g.*, on all sidebands of a modulated wave), then the resolution parameter or broadening parameter of importance so far as the demodulation effect is concerned is the ultimate or theoretical resolution, rather than the actual resolution. This appears to us to be true because the demodulation effect comes from mixing or beating between coherently related sidebands. System broadening effects which simply smear out each sideband *in the same fashion* should not affect this mixing or beating.

In addition, we argue that if a nonmonochromatic light signal is modulated by a phase modulator which modulates equally all the spectral components, then such light will still be demodulated by the proposed device. This is because each spectral component in the polychromatic wave will be given modulation sidebands. The demodulator will cause these sidebands to beat together in the fashion described above, and the resulting demodulation effects at the modulation frequency will add together coherently. There will, of course, be in addition numerous overlaps and mixings between all the polychromatic components at all frequencies, producing beats at all lower frequencies. Providing, however, that there are not coherent relationships among the polychromatic spectral components, the result of this process will be only a noise spectrum or a background noise. To first order, this noise spectrum will be accounted for by the noise formula given later in this paper, using the actual width of the light spot created by the polychromatic light input.

Therefore, we argue that the proposed demodulator does not require either a monochromatic light input or an ideal optical system, but should function properly with much less ideal conditions. However, a more complete and detailed analysis is obviously required rigorously to verify these intuitive arguments.

Optical Design Considerations

From the previous analysis, it is clear that one wants to make the distance a on the cathode between adjacent sideband spectral components as large as possible; but it is also clear that the individual spectral components should considerably overlap each other. In optical terminology, an instrument giving high dispersion and low resolution is required. As mentioned earlier, two instruments which appear to be convenient are the Michelson echelon and the Fabry-Perot interferometer.

The Michelson transmission echelon consists of a stack or staircase of staggered glass plates, as shown in Fig. 6, such that light rays passing through different plates interfere in a very high-order m. The dispersion is determined by the step height b, and the plate thickness t, together with the index of refraction n of the plates, and the resolution is determined by the number of plates. The light intensity pattern created by this instrument when operated such that only a single order is present consists of a line pattern parallel to the staircase treads with the variation transverse to each individual line following the $U(x)$ distribution of (2). The over-all line pattern lies under a broader over-all intensity distribution of the same general form.

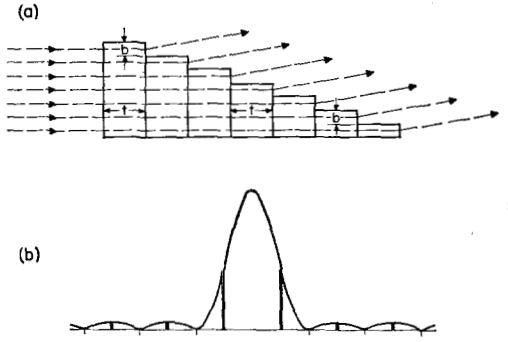

Fig. 6—(a) Michelson echelon. (b) A typical interference pattern.

As illustrated for a typical case in Fig. 6, a monochromatic input produces a series of regularly spaced lines representing interference in successively higher orders. However, as Fig. 6 illustrates, most of the light intensity goes into one or two orders lying within the central maximum. We will assume for simplicity that these orders are far enough separated compared to the sideband spacing (*cf.* below) so that the modulation sidebands cluster about each order without overlap and interference between sidebands from different orders. We will also assume that only the strongest central order lies on the photocathode, although this is by no means necessary since, if several orders are present on the photocathode, their effects will simply add.

A Fabry-Perot interferometer consists of two flat and parallel, partially reflecting plates which produce an interference pattern consisting of a set of rings. The radial variation of this set of rings is generally similar to the transverse or x variation of the echelon interference pattern, and hence the circularly symmetric type of demodulation shown in Fig. 2 becomes possible. This type of operation may offer some advantages in the design of the demodulator tube, but also appears to have some disadvantages such as light losses in the Fabry-Perot reflecting surfaces. Since the general principles are the same as in the echelon case, and since an echelon system has been selected for the initial experiments, we will not consider the Fabry-Perot system in any further detail here.

It is convenient to express optical wavelengths or frequencies in terms of the corresponding wave numbers $y = \lambda^{-1}$. The linear dispersion of a Michelson echelon, *i.e.*, the line position shift dx_0 on the cathode produce by a wave-number change dy, is then given by[1]

$$\frac{dx_0}{dy} = \frac{mf}{b}\frac{1}{y^2} \tag{17}$$

where f is the focal length, and the interference order of the central line is given by $M = (n_0 - 1)yt$. Table I shows the design parameters for a proposed experiment now in preparation, using a commercially available Michelson echelon. The coherent light source will be a ruby laser, modulated by a KDP modulator[2] at the modulation frequency $f_m = 3000$ Mc/s. The nominal phase modulation parameter $\delta = 1$ has been obtained in this modulator with a few hundred watts of modulating power. Note that for these experimental parameters, the wave-number spacing between modulation sidebands is $\Delta y_m = 0.1$ cm^{-1} and hence the spacing a between sidebands on the cathode is

$$\begin{aligned} a &= \frac{dx_0}{dy}\Delta y_m \\ &= [350 \text{ microns/cm}^{-1}][0.1 \text{ cm}^{-1}] \\ &= 35 \text{ microns}. \end{aligned} \tag{18}$$

TABLE I
Typical Design Parameters

Optical Wavelength, $\lambda = 6943$ Å ($y = \lambda^{-1} = 14{,}330$ cm^{-1})
Modulation frequency, $f_m = 3000$ Mc/s ($\Delta y_m = 0.1$ cm^{-1})
Phase modulation parameter, $\delta = \omega_d/\omega_m = 1$
Echelon step height, $b = 1$ mm
Echelon plate thickness, $t = 10$ mm
Order of interference, $m \approx 7165$
Focal length, $f = 1$ meter

For a Michelson echelon, the parameter N in $U(x)$, Eq. (2), is given by $N = \pi N' by$ where N' is the number of echelon steps within the incident light beam. For the proposed

[1] M. Born and E. Wolf, "Principles of Optics," Pergamon Press, Inc., New York, N. Y.; 1959.
[2] I. P. Kaminow, "Microwave modulation of the electro-optic effect in KH_2PO_4," *Phys. Rev. Lett.*, vol. 6, pp. 528–530; May 15, 1961.

experiment using $N' = 4$ plates, this gives $N = 180$/cm, $Na = 0.6$ radians, and a reduction factor $sinc\ Na = 0.94$. The modulation effect is thus only very slightly resolved out, but would be rapidly attenuated if a larger light beam diameter and hence more plates were used.

The spacing between adjacent orders m and $m + 1$ for an echelon is

$$\Delta x_0(m, m + 1) = \frac{\lambda f}{b} = 690 \text{ microns}. \tag{19}$$

For the experimental parameters of Table I, this yields $\Delta x_0 = 20a$, so that the requirement of no overlap between sidebands from adjacent orders is satisfied.

Wave Excitation and Signal-to-Noise Ratio

From (16) the rms transverse motion of the electron beam center of gravity is given by

$$\Delta x_{cg}^2 = \frac{\delta^2 a^2 \operatorname{sinc}^2 Na}{2}. \tag{20}$$

A transverse motion of the beam's initial position in the x direction corresponds to equal initial excitation of the positive- and negative-energy synchronous transverse waves, with each wave carrying signal power (+ or −) given by

$$P_s = \frac{\omega\omega_c I_0\, \Delta x_{cg}^2}{16n} \tag{21}$$

where $\eta = e_i m$, and ω_c = the cyclotron frequency.[3] The values in Table I together with $\omega_c = 3$ kMc and an assured beam current $I_0 = 100$ μa give a signal power $P_s = 15$ μw on each synchronous wave. This should be readily detectible. Note that a beam current $I_0 = 100$ μa presumes an incident light power of ~100 μw with a perfect photosurface, and correspondingly more with a real photosurface. The initial experiment is planned to use a very poor photosurface, but the light power available from the ruby laser will, or course, greatly exceed 100 μw.

The synchronous transverse beam waves are generally considered relatively noisy waves, since they have a large initial noise excitation arising from the finite size of the initial beam spot. There is also an initial noise excitation arising from the initial transverse velocity distribution of the electrons. We will neglect the latter in this discussion, in part because the finite size contribution is more important except for very small beam spots, and in part because the initial transverse velocity distribution will depend on a number of factors which we do not wish to explore in detail here. If it is assumed for simplicity that the electron emission occurs randomly in time and uniformly in space within a strip of width D in the x direction, then the power spectral density of the noise fluctuations in the beam's initial position is

$$\Delta x_n^2 = \frac{e\, D^2}{6I_0} \tag{22}$$

and the corresponding noise power on each synchronous wave is

$$P_n = \frac{e\omega\omega_c\, D^2 B}{96\eta}. \tag{23}$$

The actual x distribution of the emitted current is, of course, not a uniform rectangular distribution, and the width of the initial beam spot will depend upon such factors as the amount of system broadening in the optical system. If we choose as an example the relatively large spot width $D = 1$ mm, together with $f = f_c = 3000$ Mc/s and a bandwidth $B = 2$ Mc/s, the noise power is $P_n \sim 10^{-11}$ watts (corresponding to an equivalent temperature of 240,000° K). Therefore, the SNR in the proposed experiment should be at least 60 db.

With transverse velocity noise omitted, the SNR can be expressed in general as

$$\frac{P_s}{P_n} = \frac{\Delta x_{cg}^2}{\Delta x_n^2} = \frac{3I_0\, \delta^2 a^2 \operatorname{sinc}^2 Na}{e\, D^2 B}. \tag{24}$$

It should, in general, be possible to make $sinc\ Na \to 1$. Moreover, if $\delta \leq 1$ so that only the first sideband on each side is important, and if system broadening effects are not large, then the spot width will be given by $D \approx 3a$. With these assumptions, the SNR becomes

$$\frac{P_s}{P_n} = \frac{2}{3}\frac{(\delta I_0)^2}{2eI_0 B}. \tag{25}$$

In other words, for this ideal case, the signal current can be considered as $\sim\delta I_0$, and the noise can be considered as simply full shot noise. For $\delta = 1$ and any reasonable beam current, this SNR is extremely large, and hence very weak light fluxes should in principle be detectible with a good photosurface in this fashion. The SNR, of course, deteriorates for a larger spot width $D > 3a$ as noted above. In addition, as a practical matter, the design of the succeeding transverse-wave tube elements becomes very difficult if the beam current is very low. Beam currents much smaller than 100 μa require either a very long interaction region or a very-high-impedance transverse coupler to extract the signal from the synchronous waves. Our proposed experiment calls for a flattened helix transverse coupler with a center conductor, the helix being a few cm long. It should also be possible, if needed, to provide synchronous-wave amplification directly within the demodulator tube by a variety of methods well known in the microwave tube field, *e.g.*, via a dc quadrupole section. An alternative would be first to convert the synchronous waves into true cyclotron waves. after which the latter could be amplified and/or detected by well-known methods.

[3] A. E. Siegman, "Waves on a filamentary electron beam in a transverse-field slow-wave circuit," *J. Appl. Phys.*, vol. 31, pp. 17–26; January, 1960.

Appendix

The following proof is due to I. C. Chang of Stanford Electronic Laboratories:

Proof of

$$\sum_{n=0}^{\infty} (2n + 1)J_{n+m+1}(x)J_{n-m}(x) = \frac{x}{2}\,\delta_{m0}$$

where δ_{m0} = Kronecker delta symbol.

Starting with

$$\frac{2}{\pi}\int_0^{\pi/2} x \cos\theta \cos(2m + 1)\theta\, d\theta = \frac{x}{2}\,\delta_{m0}.$$

Introducing the Gegenbauer Identity

$$x \cos\theta = \sum_{n=0}^{\infty} (2n + 1)J_{2n+1}(2x \cos\theta).$$

Then

$$\frac{2}{\pi}\int_0^{\pi/2} \left[\sum_{n=0}^{\infty} (2n + 1)J_{2n+1}(2x \cos\theta)\right] \cdot \cos(2m + 1)\theta\, d\theta = \frac{x}{2}\,\delta_{m0}.$$

Using the integral form for products of Bessel functions

$$\frac{2}{\pi}\int_0^{\pi/2} J_{u+v}(2x \cos\theta) \cos(u - v)\theta\, d\theta = J_u(x)J_v(x)$$

and interchanging the summation and integration immediately gives the desired result.

Acknowledgment

The authors wish to note that an apparently very similar demodulation scheme was independently proposed by H. W. Kogelnik of the Bell Telephone Laboratories.

Subharmonic Pumping of Parametric Amplifiers*

KENNETH E. MORTENSON†, SENIOR MEMBER, IRE

Summary—**The purpose of this paper is to present in some detail the operation of a parametric amplifier pumped subharmonically as compared to being directly pumped. As considered here, subharmonic pumping does not involve harmonic pump power generation (external to the varactor) but the utilization of higher-order time-dependent capacitances to yield parametric amplification by employing, basically, only a three-frequency system.**

The analysis given here is based on an evaluation of the Fourier series representation of the time-dependent capacitance resulting from large-signal ("hard") pumping of varactors. This evaluation indicates that significant values of higher-order time-dependent capacitances suitable for parametric amplification are obtained with relative pump swings in excess of about 90 per cent. Utilizing these higher-order time-dependent capacitances, the amplifier operation for various orders of subharmonic pumping is treated, including such factors as pump power requirements, gain, and noise figure. It is shown that, under certain conditions, less pump power is required to generate the same negative conductance than with direct fundamental pumping. Furthermore, for the same pump power and fundamental pump frequency, it is determined that significant improvements in amplifier noise figure are achieved by employing subharmonic pumping, provided varactor losses are small.

From the results obtained by both analysis and experiment, it is concluded that subharmonic pumping, even without harmonic power generation, is not only feasible but can be very useful up to C-band signal frequencies with existing varactors.

* Received November 14, 1960; revised manuscript received, March 12, 1962. Portions of this paper were presented at the International Solid-State Circuits Conference; February 10–12, 1960.

† Microwave Associates, Inc., Burlington, Mass. Formerly at the General Electric Research Laboratory, Schenectady, N. Y.

I. Introduction

TO OBTAIN low-noise parametric amplifier operation, the idle frequency must be chosen to be several times the signal frequency of the amplifier provided amplifier cooling is not employed. This condition of high required idle frequency in turn generally necessitates the use of a still higher pump frequency ($f_s + f_i = f_p$). In many instances, because of the type, size, and power delivery vs frequency characteristics of pump sources available, it would be very convenient to use lower frequency pumping (*i.e.*, actual pumping at a fraction of the frequency of the effective pumping). In particular, the desire to employ present, compact, solid-state pump sources such as transistors or tunnel diodes, which are capable of providing adequate pump power in the UHF and *L*-band regions, suggests the consideration of some form of lower frequency pumping for low-noise amplifiers whose signal frequencies lie in the same frequency regions or possibly even higher.

Lower frequency pumping, which has been described by Bloom and Chang,[1,2] is, in general, a four-frequency

[1] S. Bloom and K. K. N. Chang, "Parametric amplification using low frequency pumping," *J. Appl. Phys.*, vol. 29, p. 594; March, 1958.

[2] K. K. N. Chang and S. Bloom, "A parametric amplifier using lower-frequency pumping," Proc. IRE, vol. 46, pp. 1383–1386; July, 1958.